

THE ROTATIONAL SPECTRUM AND STRUCTURE OF THE PHOSPHINE-HYDROGEN CYANIDE COMPLEX

A.C. LEGON and L.C. WILLOUGHBY

*Christopher Ingold Laboratories, Department of Chemistry, University College London,
20 Gordon Street, London WC1H 0AJ, UK*

Received 21 October 1983

The rotational spectrum of the weakly bound complex (PH_3 , HCN) in its vibrational ground state has been observed by the technique of pulsed-nozzle, Fourier-transform microwave spectroscopy. The isotopic species (PH_3 , HC^{14}N), (PH_3 , DC^{14}N) and (PH_3 , HC^{15}N) exhibit spectra of the symmetric-top type from which accurate values of the spectroscopic constants B_0 , D_J , D_{JK} and χ_{aa} (^{14}N) have been determined. For (PH_3 , HC^{14}N) the appropriate values are: $B_0 = 1553.3709(1)$ MHz, $D_J = 3.306(3)$ kHz, $D_{JK} = 256.9(6)$ kHz and $\chi_{aa} (^{14}\text{N}) = -4.3591(14)$ MHz. The geometry of the complex established from the spectroscopic constants is one of C_{3v} symmetry at equilibrium, with the HCN molecule lying along the C_3 axis of PH_3 and oriented so that it forms a hydrogen bond to the P atom. The effective distance from P to the C nucleus is $r(\text{P} \cdots \text{C}) = 3.913$ Å.

1. Introduction

Rotational spectroscopy is now established [1] as a powerful method by which the properties of effectively isolated, weakly bound molecular complexes can be determined. Conventional microwave spectroscopy of equilibrium gas mixtures is effective for hydrogen bonded complexes of the stronger type but for weaker complexes a sufficient number density cannot be achieved by cooling such mixtures. On the other hand, the techniques that involve supersonic expansion of a mixture of the components seeded in argon gas lead, even for the most weakly bound complexes, to a high number density at a very low effective temperature. These techniques thus have a high sensitivity for molecular complexes and we have used one of them (pulsed-nozzle, Fourier-transform microwave spectroscopy) in a series of investigations into weakly bound complexes formed by phosphine with the hydrogen halides [2-4]. Not only have such species thereby been identified unambiguously in the gas phase but also important properties of the complexes have been established.

We now report a detailed identification and characterisation of a molecular complex formed by phosphine with hydrogen cyanide, the hydride of

the pseudohalogen $(\text{CN})_2$. From an investigation of the rotational spectrum, we have determined accurate values of the rotational constant, centrifugal distortion constants and (where appropriate) the ^{14}N -nuclear quadrupole coupling constant for the isotopic species (PH_3 , HC^{14}N), (PH_3 , DC^{14}N), (PH_3 , HC^{15}N) and (PH_2D , HC^{14}N). The form of the observed spectra and the detailed magnitude of the rotational constants allow the definite conclusion that the complex has C_{3v} symmetry at equilibrium, with the HCN axis lying along the C_3 axis of PH_3 and both subunits oriented so that the H atom of HCN forms a hydrogen bond to the P atom of PH_3 . Analyses of the ^{14}N -nuclear quadrupole coupling constants and the centrifugal distortion constants lead to conclusions about the motion of the HCN subunit within the complex and the strength of the hydrogen bond.

2. Experimental

Rotational spectra of (PH_3 , HCN) were detected in the vibrational ground state by using a pulsed-nozzle Fourier-transform microwave spectrometer of the type described by Balle and Flygare [5]. A preliminary description of the spectrometer

at University College has been given elsewhere [2].

The gas mixture pulsed from the nozzle (0.7 mm orifice) into the Fabry-Perot cavity was made as follows. Hydrogen cyanide gas was admitted to the evacuated, stainless steel reservoir at a pressure of ≈ 10 Torr and the majority removed by condensation. A partial pressure of ≈ 25 Torr of phosphine was then added and the whole mixture diluted with argon to a total pressure of 1 atm.

Phosphine was supplied by Matheson Inc., or prepared by the action of 6 M sulphuric acid on aluminium phosphide [6] in vacuo. In the latter case, the product was initially condensed at liquid-nitrogen temperature together with considerable water. A sufficiently dry product was obtained by distillation of the crude condensate from a Drikold/acetone mixture at ≈ 200 K. PH_2D was prepared by a similar procedure but using an appropriate $\text{H}_2\text{SO}_4/\text{D}_2\text{SO}_4$ mixture. Hydrogen cyanide and deuterium cyanide were prepared by the action of phosphoric and perdeuterophosphoric acids respectively on potassium cyanide in vacuo. For HC^{15}N , an isotopically enriched (95%) sample of KC^{15}N was employed.

3. Results

3.1. Nature of observed spectra and magnitude of the spectroscopic constants

The rotational spectrum attributed to the complex formed by phosphine and hydrogen cyanide is characteristic of the vibrational ground state of a symmetric-top molecule in which an ^{14}N nucleus lies on the symmetry axis. Thus, it consists of series of equally spaced transitions ($J+1, K \leftarrow J, K$), with each transition exhibiting the required ^{14}N -nuclear quadrupole hyperfine pattern. Figs. 1 and 2 show three nuclear quadrupole components of the $J=3 \leftarrow 2, K=0$ transition of $(\text{PH}_3, \text{HC}^{14}\text{N})$ which are sufficiently close in frequency to be observed simultaneously within the bandwidth of the Fabry-Perot cavity. Each component appears as a doublet in fig. 2 because of a Doppler effect whose origin has been fully discussed [5]. Observed transition frequencies for $1 \leq J \leq 4$ are given

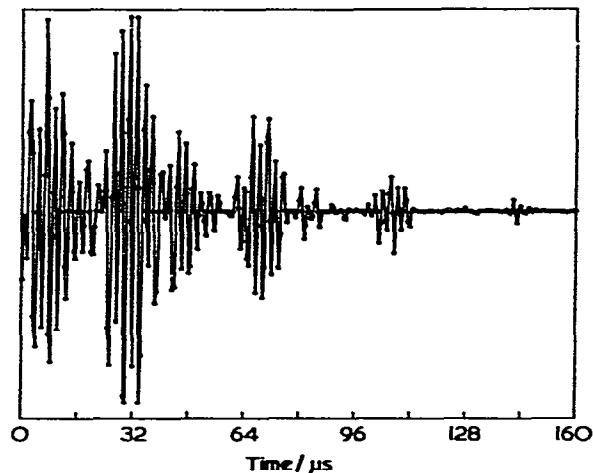


Fig. 1. Transient emission signal arising from the $F=2 \leftarrow 1, 3 \leftarrow 2$ and $4 \leftarrow 3$ components of the $J=3 \leftarrow 2, K=0$ transition of $(\text{PH}_3, \text{HC}^{14}\text{N})$ digitized at a rate of $0.5 \mu\text{s}/\text{point}$. The polarizing radiation has a frequency of 9319.4317 MHz. The emission from ≈ 10 gas pulses was averaged to yield this signal.

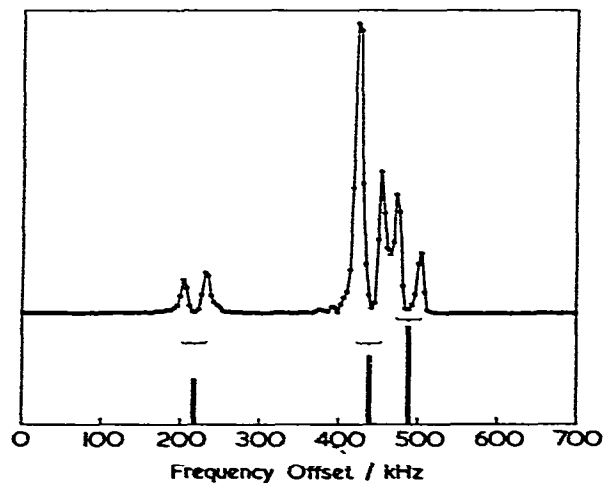


Fig. 2. Power spectrum resulting from the Fourier transformation of the time-domain signal of fig. 1. Frequencies are offset at a rate of 3.90625 kHz/point from 9319.4317 MHz. The transitions are each split into a doublet, as indicated, by a Doppler effect and are assigned, in order of increasing offset, as the $F=2 \leftarrow 1, 3 \leftarrow 2$ and $4 \leftarrow 3$ ^{14}N -nuclear quadrupole components of the $J=3 \leftarrow 2, K=0$ transition, respectively, in $(\text{PH}_3, \text{HC}^{14}\text{N})$. The reason for the discrepancy between the observed and calculated intensities of hyperfine components lies in the rapid variation of the response curve of the high Q Fabry-Perot cavity with frequency.

Table 1
Observed and calculated rotational transition frequencies of (PH₃, HC¹⁴N)

Transition <i>J' F' ← J'' F''</i>	<i>K</i> = 0			<i>K</i> = 1		
	<i>ν</i> _{obs} (MHz)	<i>ν</i> _{calc} (MHz)	diff.(kHz)	<i>ν</i> _{obs} (MHz)	<i>ν</i> _{calc} (MHz)	diff.(kHz)
2 2 ← 1 2	6212.0700	6212.0701	-0.1	(6211.9017) ^{a)}	6211.9144	(-12.7)
2 1 ← 1 0	6212.2873	6212.2882	-0.9	(6213.9989)	6213.9870	(11.9)
2 2 ← 1 1	6213.3769	6213.3777	-0.8	(6211.2597)	6211.2601	(-0.4)
2 3 ← 1 2	6213.4719	6213.4712	0.7	(6212.6033)	6212.6154	(-12.1)
2 1 ← 1 1	6215.5574	6215.5576	-0.2	(6212.3480)	6212.3513	(-3.3)
3 3 ← 2 3	- ^{b)}	9318.4669	-	9317.3532	9317.3531	0.1
3 2 ← 2 1	9319.6503	9319.6502	0.1	9318.4351	9318.4358	-0.7
3 3 ← 2 2	9319.8693	9319.8682	1.1	9318.0504	9318.0543	-3.9
3 4 ← 2 3	9319.9209	9319.9201	0.8	9318.4520	9318.4439	8.1
3 2 ← 2 2	9321.8291	9321.8300	-0.9	9319.5215	9319.5271	-5.6
4 4 ← 3 4	12424.6669	12424.6677	-0.8	12422.8634	12422.8654	-2.0
4 3 ← 3 2	12426.0265	12426.0272	-0.7	12424.0824	12424.0729	9.5
4 4 ← 3 3	12426.1194	12426.1207	-1.3	12423.9555	12423.9561	-0.6
4 5 ← 3 4	12426.1568	12426.1537	3.1	12424.1266	12424.1296	-3.0
4 3 ← 3 3	12427.9887	12427.9890	-0.3	12425.5444	12425.5457	-1.3
5 5 ← 4 5	15530.5680	15530.5697	-1.7	15528.1623	15528.1668	-4.5
5 4 ← 4 3	15532.0025	15532.0038	-1.3	15529.4799	15529.4778	2.1
5 5 ← 4 4	15532.0596	15532.0557	3.9	15529.4323	15529.4311	1.2
5 6 ← 4 5	15532.0790	15532.0786	0.4	15529.5271	15529.5260	1.1
5 4 ← 4 4	15533.8707	15533.8721	-1.4	15531.0665	15531.0674	-0.9

^{a)} Transition frequencies enclosed in parentheses were not included in the least-squares analysis. See text for discussion.

^{b)} This transition is obscured by the much stronger $F = 4 \leftarrow 3$ component of the $J = 3 \leftarrow 2$, $K = 1$ transition.

in table 1 for (PH₃, HC¹⁴N). Those for transitions associated with $K = 0$ are recorded in a separate column from those for transitions having $K = 1$. We did not observe spectra originating in states with $K \geq 2$ because of the low effective temperature (≈ 5 K) of the supersonically expanded gas. $K = 2$ states will be higher in wavenumber by ≈ 16 cm⁻¹ than the corresponding $K = 0$ states because the value of the rotational constant A_0 of the complex will be of similar magnitude to that associated with the symmetry axis of free PH₃ [7]. Consequently, such states will be negligibly populated. For similar reasons, all observed spectra have been assigned to the vibrational ground state of the complex.

The frequencies given in table 1 were fitted in a standard non-linear least-squares analysis to give spectroscopic constants by use of the hamiltonian

$$H = H_R + H_Q, \quad (1)$$

where H_R is the usual effective rotational hamiltonian of a symmetric-top molecule with eigenvalues

$$E_R = B_0 J(J+1) - D_J J^2(J+1)^2 - D_{JK} J(J+1)K^2. \quad (2)$$

The term H_Q describes the hyperfine splitting arising from the interaction of the ¹⁴N-nuclear electric quadrupole moment with the electric field gradient at the ¹⁴N nucleus and is written

$$H_Q = -\frac{1}{6} \mathbf{Q} : \nabla \mathbf{E}, \quad (3)$$

where \mathbf{Q} and $\nabla \mathbf{E}$ are the nuclear electric quadrupole tensor and the electric field gradient tensor, respectively. The matrix of H was set up in the $J + I = F$ basis, in which H_R has only the diagonal elements given in eq. (2) and in which the only non-zero elements of H_Q are of the type $\langle J, K, I, F | H_Q | J', K, I, F \rangle$, where $J' = J, J \pm 1$,

$J \pm 2$ [8]. For a symmetric-top molecule having the quadrupolar nucleus on the symmetry axis (a), the observed hyperfine pattern is determined entirely by the single nuclear quadrupole coupling constant $\chi_{aa} = -eQ(\partial^2 V/\partial a^2)$. The determined spectroscopic constants B_0 , D_J , D_{JK} and χ_{aa} are recorded in table 2. Frequencies calculated in the final cycle of the least-squares treatment and the corresponding residuals are included in table 1.

We note that rather than fit all transitions in a single analysis, we have treated the $K=0$ set separately from the $K=1$ set. Hence, two values, $\chi_{aa}(K=0)$ and $\chi_{aa}(K=1)$, of the ^{14}N -nuclear quadrupole coupling constant were determined and ($B_0 - D_{JK}$) instead of B_0 results for $K=1$ transitions. This separate fitting procedure was suggested by our experience with $(\text{PH}_3, \text{HBr})$ [4], for which $\chi_{aa}(K=0)$ and $\chi_{aa}(K=1)$ differ significantly. In the present case, however, the two quantities are identical within experimental error (table 2).

There is another reason for fitting $K=0$ and $K=1$ transitions separately. Components of the $J=2 \leftarrow 1$, $K=1$ transitions exhibited a small (≈ 20 kHz) additional splitting and this splitting led to errors in the frequencies that were larger than the usual 1 kHz. This substructure was either absent or negligible for $K=1$ transitions of higher J and absent in all $K=0$ transitions. Similarly, for the isotopic species $(\text{PH}_3, \text{HC}^{15}\text{N})$ in which nuclear quadrupole coupling is absent, the effect was important only in the $J=2 \leftarrow 1$, $K=1$ transi-

tion. Undoubtedly, the extra structure arises from nuclear-spin interactions involving the four $J=1/2$ nuclei of the PH_3 subunit but even for $J=2 \leftarrow 1$ it is not sufficiently well-resolved to analyse. Such effects are likely to be most serious at low J and high K . Accordingly, the $J=2 \leftarrow 1$, $K=1$ transitions have been excluded from the least-squares fit (see table 1). Even so, we note that the fit for the $K=1$ set of transitions is considerably worse than that for the $K=0$ set as a result of the effect described.

Observed and calculated frequencies for the $J=4 \leftarrow 3$ and $5 \leftarrow 4$ transitions of the species $(\text{PH}_3, \text{DC}^{14}\text{N})$ are recorded in table 3. Again, $K=0$ and $K=1$ transitions were treated separately, with the results for the spectroscopic constants shown in table 2. The presence of the axial D nucleus ($J=1$) manifested itself in a slight splitting of some of the ^{14}N -nuclear quadrupole components even in the $J=4 \leftarrow 3$ transition and hence, because such effects increase rapidly as J decreases, precluded the useful measurement of lower J transitions. Results for the species $(\text{PH}_3, \text{D}, \text{HC}^{15}\text{N})$ are similarly given in tables 4 and 5. Examination of table 4 indicates that no $K=1$ transitions were observed for this species. A careful search in the predicted frequency regions failed to reveal such $K=1$ transitions and indicates that they are weaker than expected. A similar result obtains for $(\text{PH}_3, \text{HBr})$ [4] and (PH_3, HF) [5] but its origin is not completely understood. The constants ($B_0 + C_0$) and D_0 recorded in table 2

Table 2
Spectroscopic constants of various isotopic species of $(\text{PH}_3, \text{HC}^{14}\text{N})$

Transition	B_0 (MHz)	$(B_0 - D_{JK})$ (MHz)	D_J (kHz)	D_{JK} (kHz)	χ_{aa} (kHz)
$J=4 \leftarrow 3$	110 170.1	110 169.5	11.0	11.0	4 110.16
$J=5 \leftarrow 4$	110 170.1	110 169.5	11.0	11.0	4 110.16
$J=3 \leftarrow 2$	110 170.1	110 169.5	11.0	11.0	4 110.16
$J=2 \leftarrow 1$	110 170.1	110 169.5	11.0	11.0	4 110.16
$J=4 \leftarrow 3$	110 170.1	110 169.5	11.0	11.0	4 110.16
$J=5 \leftarrow 4$	110 170.1	110 169.5	11.0	11.0	4 110.16

^a B_0 and $(B_0 - D_{JK})$ transition band separated. All are fit constants.

^b B_0 transition not observed. All are fit constants.

^c B_0 and $(B_0 - D_{JK})$ transition band overlapped.

Table 3
Observed and calculated rotational transition frequencies of $(PH_3, DCN)_2$

Transition $J, K_1, K_2 \rightarrow J', K_1', K_2'$	$K_1 = 0$ transitions			$K_1 = 1$ transitions		
	ν_{obs} (MHz)	ν_{calc} (MHz)	diff. (MHz)	ν_{obs} (MHz)	ν_{calc} (MHz)	diff. (MHz)
4 ₀ 4 ₀ 4 ₀ → 3 ₁ 3 ₀ 4 ₀	12391.9628	12391.9647	-1.9	12392.7952	12392.798	-2.8
4 ₀ 4 ₀ 4 ₀ → 3 ₁ 3 ₀ 4 ₁ 3 ₂	12392.2721	12392.2722	-0.1	12393.1047	12393.105	-0.3
4 ₀ 4 ₀ 4 ₀ → 3 ₁ 3 ₀ 4 ₁ 3 ₁	12392.5817	12392.5818	-0.1	12393.4142	12393.414	-0.2
4 ₀ 4 ₀ 4 ₀ → 3 ₁ 3 ₀ 4 ₁ 3 ₀	12392.8912	12392.8913	-0.1	12393.7237	12393.723	-0.7
4 ₀ 4 ₀ 4 ₀ → 3 ₁ 3 ₀ 4 ₁ 3 ₀	12393.2008	12393.2009	-0.1	12394.0332	12394.033	-0.2
4 ₀ 4 ₀ 4 ₀ → 3 ₁ 3 ₀ 4 ₁ 3 ₀	12393.5103	12393.5104	-0.1	12394.3427	12394.342	-0.7
4 ₀ 4 ₀ 4 ₀ → 3 ₁ 3 ₀ 4 ₁ 3 ₀	12393.8198	12393.8199	-0.1	12394.6522	12394.652	-0.2

^a Observed ν_{obs} overlap with the Doppler doublet component of adjacent transition.

Table 4
Observed and calculated rotational transition frequencies of $(PH_3, DCN)_2$

Transition $J, K_1, K_2 \rightarrow J', K_1', K_2'$	ν_{obs} (MHz)		
	ν_{obs} (MHz)	ν_{calc} (MHz)	diff. (MHz)
4 ₀ 4 ₀ 4 ₀ → 3 ₁ 3 ₀ 4 ₀	12391.9628	12391.9647	-1.9
4 ₀ 4 ₀ 4 ₀ → 3 ₁ 3 ₀ 4 ₁ 3 ₂	12392.2721	12392.2722	-0.1
4 ₀ 4 ₀ 4 ₀ → 3 ₁ 3 ₀ 4 ₁ 3 ₁	12392.5817	12392.5818	-0.1
4 ₀ 4 ₀ 4 ₀ → 3 ₁ 3 ₀ 4 ₁ 3 ₀	12392.8912	12392.8913	-0.1
4 ₀ 4 ₀ 4 ₀ → 3 ₁ 3 ₀ 4 ₁ 3 ₀	12393.2008	12393.2009	-0.1
4 ₀ 4 ₀ 4 ₀ → 3 ₁ 3 ₀ 4 ₁ 3 ₀	12393.5103	12393.5104	-0.1
4 ₀ 4 ₀ 4 ₀ → 3 ₁ 3 ₀ 4 ₁ 3 ₀	12393.8198	12393.8199	-0.1

Table 5
Observed and calculated rotational transition frequencies of $(PH_3, DCN)_2$

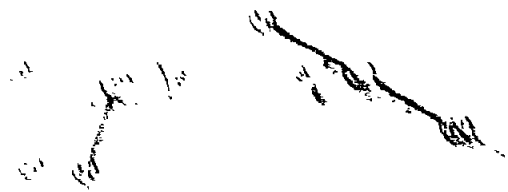
Transition $J, K_1, K_2 \rightarrow J', K_1', K_2'$	ν_{obs} (MHz)		
	ν_{obs} (MHz)	ν_{calc} (MHz)	diff. (MHz)
4 ₀ 4 ₀ 4 ₀ → 3 ₁ 3 ₀ 4 ₀	12391.9628	12391.9647	-1.9
4 ₀ 4 ₀ 4 ₀ → 3 ₁ 3 ₀ 4 ₁ 3 ₂	12392.2721	12392.2722	-0.1
4 ₀ 4 ₀ 4 ₀ → 3 ₁ 3 ₀ 4 ₁ 3 ₁	12392.5817	12392.5818	-0.1
4 ₀ 4 ₀ 4 ₀ → 3 ₁ 3 ₀ 4 ₁ 3 ₀	12392.8912	12392.8913	-0.1
4 ₀ 4 ₀ 4 ₀ → 3 ₁ 3 ₀ 4 ₁ 3 ₀	12393.2008	12393.2009	-0.1
4 ₀ 4 ₀ 4 ₀ → 3 ₁ 3 ₀ 4 ₁ 3 ₀	12393.5103	12393.5104	-0.1
4 ₀ 4 ₀ 4 ₀ → 3 ₁ 3 ₀ 4 ₁ 3 ₀	12393.8198	12393.8199	-0.1

Observed ν_{obs} overlap with the Doppler doublet component of adjacent transition.

... ..

... ..

... ..



... ..

... ..

... ..

... ..

...
...
...
...
...

... ..

[REDACTED]

[REDACTED]

[REDACTED]

In the circumstances in which the [REDACTED] [REDACTED] and [REDACTED] [REDACTED] of the [REDACTED] are [REDACTED] [REDACTED] [REDACTED] and

[REDACTED]

[REDACTED]

[REDACTED]

[REDACTED]

